The broadening of the satellite reflections in the nonideal superlattice model

1990 J. Phys.: Condens. Matter 2 265

(http://iopscience.iop.org/0953-8984/2/2/002)

J. Phys.: Condens. Matter 2 (1990) 265–272. Printed in the UK

The broadening of the satellite reflections in the non-ideal superlattice model

M Wójcik, J Sass and J Gaca
Institute of Electronic Materials Technology, ul. Wolczynska 133, 01919 Warsaw, Poland

Received 3 October 1988, in final form 9 May 1989

Abstract. A model of coherently diffracting domains with sinusoidal composition modulation waves that have a different wavelength in each domain is presented. Formulae describing the summed x-ray intensities diffracted independently by each domain are derived in the kinematical case. The model is experimentally verified for the alloy Alnico, in which a gaussian distribution of the modulation wavelength is assumed. The broadening of the satellite reflections in relation to the nodal reflection and the non-linear dependence of the half-width of the satellite reflection on its order are shown for this case.

1. Introduction

The kinematical theory of diffraction in superlattices (SL) has shown that [1, 2], for an ideal SL model with periodical modulation waves, the half-widths of the satellite and nodal reflections are identical. In the ideal SL model it is assumed that in the entire area of the crystal there is one strictly definite modulation wavelength. The modulation wave may have any shape provided the periodicity is preserved.

In our previous work [3] it was shown that the best fit between the theoretical and experimental intensity spectra is obtained when the satellite's half-widths are greater than that of the nodal reflection. This was an arbitrary assumption and only a brief explanation of what could cause such behaviour was offered. It is known [2, 4–6] that if there is a chemical gradient across the sample, then there will be a distribution of modulation wavelength around some average value: this is reflected in the widths of the satellite reflections. The aims of this paper are: to formulate a model based on some ideas contained in reference [2]; to explain the broadening of the satellite reflections; to derive a formula based on this model describing the diffraction intensity spectrum in the kinematical case; and to provide experimental verification of the model. The proposed formula is in a simple way related to the de Fontain formula [1] for an ideal SL.

2. Model of the coherent scattering domains

Let there be a chemical gradient across the crystal, which implies dividing it into coherent scattering domains (CSD). In each CSD the composition modulation wave can be described by means of the sinusoidal wave. The wavelength Λ_i in each CSD is constant but it may differ from one CSD to another. The variation of the composition in each CSD is coupled

0953-8984/90/020265 + 08 $03.50

to a structure factor and the lattice constant modulation [3, 9]. The CSDs are separated by the boundaries in such a way that there is no long-range order in the lateral direction of the crystal. Each CSD has a sub-microscopic lateral diameter D ($D = Na$, where $N \approx 10^4$ and a is the mean value of the lattice parameter over the whole crystal). The x-ray penetration depth is much larger than the modulation wavelength.

For convenience, let us assume that the CSDs are so numerous that the use of a continuous probability distribution $N(\Lambda)$ describing the appearance frequency of a modulation wave with wavelength $\Lambda \in (\Lambda, \Lambda + d\Lambda)$ in some CSD is reasonable. In this model it is assumed that the parameters $\Delta a/a$ and η_h do not depend on Λ_i and are constant over the whole crystal.

The theory of diffraction for an ideal SL model may be used in any CSD in which compositional modulation exists. As was shown in reference [6], the observed intensity spectrum arising from the given CSD in the vicinity of the nodal reflection ($h00$) can be described by the expression

$$g^h(\theta, \Lambda) = A\left[J_0^2(hx)\rho_0^h(\theta) + \sum_{\substack{L=-\infty \\ L\neq 0}}^{\infty} J_L^2(hx)\left(1 - L\frac{\eta_h}{hx}\right)^2 \rho_L^h(\theta, \Lambda)\right] \tag{1a}$$

where

$$A = (D/a)^2 f_h^2. \tag{1b}$$

x is a parameter linking the lattice (a, Δa) and superlattice (Λ) parameters:

$$x = (\Lambda\Delta a)/a^2. \tag{1c}$$

Δa is the amplitude of the lattice constant modulation; f_h is the average structure factor; J_L is the Lth-order Bessel function; h is Miller's index; η_h is the relative amplitude of the structure factor modulation; θ is the angular coordinate; $\rho_0^h(\theta)$ is the function describing the profile of the nodal reflection; and $\rho_L^h(\theta, \Lambda)$ is the function describing the profile of the Lth satellite reflection.

It follows from the CSD model of the crystal that the total intensity is a sum of the partial intensities diffracted by each CSD. Treating $g^h(\theta, \Lambda)$ as a contribution from all CSDs for which the modulation wavelength Λ is contained in the interval (Λ, $\Lambda + d\Lambda$), one obtains the expression describing the total intensity spectrum in the form

$$G^h(\theta) = \int_0^{\infty} N(\Lambda) g^h(\theta, \Lambda)\, d\Lambda. \tag{2}$$

Equations (1) and (2) give:

$$G^h(\theta) = G_0^h(\theta) + \sum_{\substack{L=-\infty \\ L\neq 0}}^{\infty} G_L^h(\theta) \tag{3}$$

where

$$G_0^h(\theta) = A\rho_0^h(\theta)\left(\int_0^{\infty} J_0^2(h\Delta a\Lambda/a^2) N(\Lambda)\, d\Lambda\right) \tag{4}$$

and

$$G_L^h(\theta) = A\int_0^{\infty} J_L^2(h\Delta a\Lambda/a^2) N(\Lambda)\left(1 - L\frac{\eta_h a^2}{h\Delta a\Lambda}\right)^2 \rho_L^h(\theta, \Lambda)\, d\Lambda. \tag{5}$$

From equations (4) and (5) there follows a broadening of the satellite reflection profiles described by $G_L^h(\theta)$, in relation to the nodal reflection described by $G_0^h(\theta)$. This occurs because the total intensity is a sum of the partial intensities from the different CSDs, and every possible contribution has a different location on the 'θ' scale.

The contribution from some CSD with modulation wavelength belonging to the interval $(\Lambda, \Lambda + d\Lambda)$ appears on the 'θ' scale in such a way that the location of its gravity centre is given by the relation $\theta = L\lambda/2\Lambda$.

3. Application of the CSD model to the alloy Alnico

Two basic problems should be specified when applying CSD theory to materials. The first is choosing the reflection shape from those which are used in practise. In the case of the alloy Alnico under investigation, the best results were obtained when a gaussian shape was used. This was arrived at using the Alnico sample without any modulation.

Taking into account both spectral components $K\alpha_1$ and $K\alpha_2$, the functions describing the shape of the nodal and satellite reflections are as follows.

(*a*) For the nodal reflection:

$$\rho_0^h(\theta) = \sigma_0^h\sqrt{\pi/4\ln 2}\left(\exp[-4\ln 2(\theta/\sigma_0^h)^2] + 0.5\exp[-4\ln 2((\theta-\Delta)/\sigma_0^h)^2]\right) \tag{6a}$$

(*b*) for the satellite reflections:

$$\rho_L^h(\theta, \Lambda) = \rho_0^h(\theta - L\lambda/2\Lambda) \tag{6b}$$

where σ_0^h are the half-widths of the profiles, Δ is the angular distance between the spectral components $K\alpha_1$ and $K\alpha_2$, and $L\lambda/2\Lambda$ is the centre-of-gravity position of the Lth satellite reflection (for simplicity the position of the nodal reflection gravity centre was accepted as zero).

The second problem is that the distribution $N(\Lambda)$ should be assumed taking into account the real structure of the Alnico crystal being investigated, which imposes limitations on the class of possible modulation wavelengths. As was first noted by Hillert [7], there exists critical wavelengths Λ_c of the modulation wave below which the interfacial energy in the system would be too great to permit a spinodal decomposition. Therefore modulations with wavelengths $\Lambda < \Lambda_c$ should be excluded.

On the other hand, on annealing an initially homogeneous binary solution a number of modulations with $\Lambda > \Lambda_c$ will develop, the most favoured being the one for which $\Lambda = \sqrt{2}\Lambda_c$ [8]. Taking this suggestion into account, and because of the existence of clearly marked satellite reflections in the observed experimental XRD spectrum (figure 1(*a*)) the assumption that the crystal has a property that almost all modulation wavelengths are symmetrically clustered near some favoured value seems valid. In this case modulation wavelengths which are too long may be neglected as they are not required. Therefore for further consideration the modified gaussian distribution with an appropriate dispersion was chosen in the form:

$$N(\Lambda) = B\,H(\Lambda)\sigma_\Lambda\sqrt{\pi/4\ln 2}\exp\{-4\ln 2[(\Lambda - \Lambda_0)/\sigma_\Lambda]^2\} \tag{7a}$$

where σ_Λ is the half-width of the wavelength distribution, Λ_0 is the mean value of the modulation wavelegth, B is the normalisation constant and

$$H(\Lambda) = \begin{cases} 1 & b_1 < \Lambda < b_2 \\ 0 & \text{elsewhere} \end{cases} \tag{7b}$$

where $0 < \Lambda_c < b_1 < b_2$. The function $H(\Lambda)$ defined in (7*b*) express mathematically the conditions related to the above-mentioned limitations of the range of Λ values.

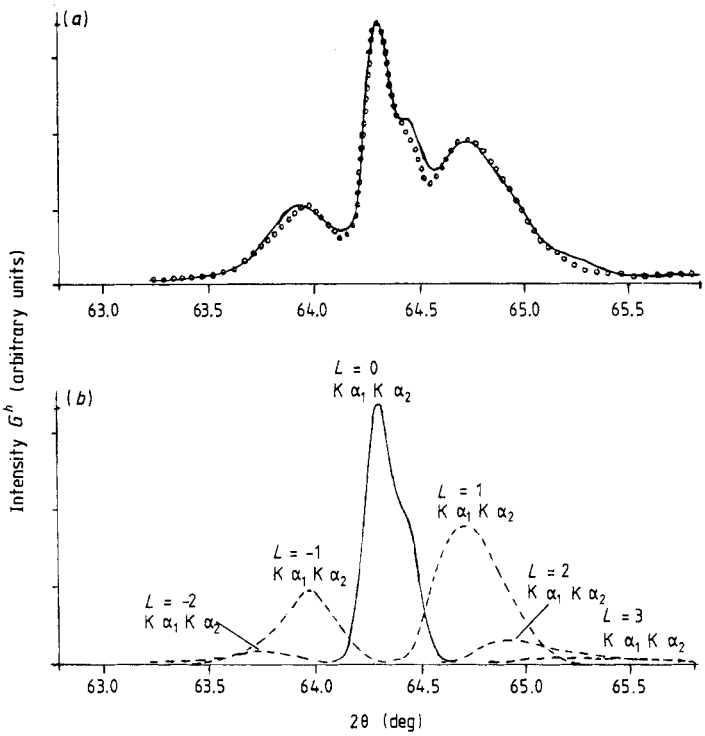

Figure 1. (*a*) Intensity spectra, reflection (200): full curve, experimental; points, theoretical. (*b*) The components of the theoretical intensity spectrum of part (*a*) for $|L| < 3$: full curve, nodal reflection; broken curves, satellite reflections.

Inserting equations (4) and (5) into (3) and using the expressions (6*a*) and (6*b*) describing the nodal and satellite reflection profiles, as well as expression (7*a*) describing the modulation wavelength distributions, the final equation describing the intensity spectrum in the vicinity of the nodal reflection ($h00$) is obtained in the form

$$G^h(\theta) = C[(\exp[-4\ln 2(\theta/\sigma_0^h)^2] + 0.5\exp\{-4\ln 2[(\theta-\Delta)/\sigma_0^h]^2\})$$
$$\times \int_{b_1}^{b_2} J_0^2(h\Delta a\Lambda/a^2)\exp\{-4\ln 2[(\Lambda-\Lambda_0)/\sigma_\Lambda]^2\}\mathrm{d}\Lambda$$
$$+ \sum_{\substack{L=-\infty \\ L=0}}^{\infty} \int_{b_1}^{b_2} J_L^2(h\Delta a\Lambda/a^2)\left(1 - L\frac{\eta_h a^2}{h\Delta a\Lambda}\right)^2 \exp\{-4\ln 2[(\Lambda-\Lambda_0)/\sigma_\Lambda]^2\}$$
$$\times (\exp\{-4\ln 2[(\theta - L\lambda/2\Lambda)/\sigma_0^h]^2\}$$
$$+ 0.5\exp\{-4\ln 2[(\theta - L\lambda/2\Lambda - \Delta)/\sigma_0^h]^2\})\,\mathrm{d}\Lambda] \qquad (8)$$

where

$$C = A\sigma_\Lambda\sigma_0^h\pi/4\ln 2.$$

It can be shown that in the limiting case, when σ_Λ tends to zero, the distribution $N(\Lambda)$ described by (7*a*) becomes Dirac delta type. In this case the integration in equation (8)

can be easily performed. As a result equation (1) is obtained, describing the case of an ideal SL model in a whole crystal.

4. Experimental procedure

The model presented in the previous section was checked experimentally by means of diffractometric investigations, using samples of Alnico alloys containing the following elements (in wt%): 8.1 Al, 14.4 Ni, 32.4 Co, 3.09 Ti, 3.28 Cu, 0.16 S, 0.23 Si, 0.062 Mn, 0.025 C, 0.07 Nb, 37.3 Fe. The samples were subjected to heat treatment as follows: homogenisation at 1260 °C for 30 min with solutioning during cooling in compression air stressing; isothermal annealing in an external magnetic field of 320 kA m^{-1} at 840 °C for 15 min. The annealing temperature was established during previous investigations: multi-stage low-temperature annealing at 650 °C for 6 h plus 600 °C for 12 h plus 550 °C for 24 h (total treatment time is 42 h). After this processing, the alloy had attained its maximum magnetic properties for the given composition (i.e. a high coercive state). Such heat treatment also brings about chemical homogeneity within the sample. Increased grain sizes up to 600 μm were observed [10].

Since, in order to check the model, a comparison of the half-widths of the nodal and satellite reflections is needed, it is essential to have a non-zero nodal reflection. In the case of the sinusoidal modulation wave, the intensity relations between the nodal and successive satellite reflections are determined by the parameter x (see equation (1*b*)). For some values of x the nodal reflection may disappear [11]. On the other hand, the smaller the value of x, the better the separation between the angular positions of the satellites, provided Δa is held fixed. Taking all this into account the sample with $x = 0.7$ was chosen for the experimental verification, which ensures both optimal intensity relations and angular separations between the nodal and satellite reflections.

An isolated grain (600 μm in size) was investigated and the data were collected with an automated diffractometer (Cu K_α radiation, 1200 W, pyrolytic graphite monochromator before the counter and pulse-height discriminator). The observed profile was measured in steps of 0.01° of 2θ, from $2\theta^{\min} = 63°$ to $2\theta^{\max} = 66°$, in the fixed-count mode. The number of counts was established as 10^4. The counting time varied from 7 to 65 s per point.

The background intensity was measured at ten points far below and ten points far above the peak region. A linear background was fitted to these data and then substracted from the observed intensities.

The exact angular positions of the local maxima were calculated by means of an analytical approximation of the experimental intensity data in the following way. Let X denote the angular range comprising the experimental profile:

$$X: = \{2\theta : 2\theta^{\min} \leqslant 2\theta \leqslant 2\theta^{\max}\}$$

where $2\theta^{\min}$ and $2\theta^{\max}$ are defined above. This angular range was divided into N sub-ranges X_L:

$$X_L: = \{2\theta : 2\theta_L^{\min} \leqslant 2\theta \leqslant 2\theta_L^{\max}, 0 \leqslant L \leqslant N\}$$

so that $X_L \cap X_{L+1} \neq \varnothing$ for each L. Each X_L was chosen so as to comprise one local maximum of the experimental profile. The least-squares method was applied to obtain

Table 1. The parameters giving the best fit for the investigated sample, reflection (200).

Superlattice parameters			Half-widths of gaussian functions	
Mean value of the modulation wavelength, Λ_0 (Å)	Amplitude of the lattice constant modulation, Δa (Å)	Relative amplitude of the structure factor modulation, η_h	Approximately describing the distribution $N(\Lambda)$, σ_Λ (Å)	Approximately describing the standard profile of nodal reflection, σ_0 (deg)
201	0.033	−0.26[a]	60.0	0.0935

[a] The minus sign denotes that the structure factor has a maximum in the areas where the lattice parameter reaches its minimum.

the polynomial function $K_L(2\theta)$ approximating the experimental profile after background correction in each sub-range X_L. The analytical function $F(2\theta)$ describing the profile over the whole range is defined as follows:

$$F(2\theta) = \begin{cases} K_L(2\theta) & 2\theta \in X_L - X_{L+1} - X_{L-1} \\ L_L(2\theta) & 2\theta \in X_L \cap X_{L+1} \end{cases}$$

where $X_0 = X_{N+1} = \varnothing$ and

$$L_L(2\theta) = (\theta_L^{\max} - \theta)/(\theta_L^{\max} - \theta_{L+1}^{\min})K_L(2\theta) + (\theta - \theta_{L+1}^{\min})/(\theta_L^{\max} - \theta_{L+1}^{\min})K_{L+1}(2\theta)$$

and $2\theta^{\min} \leqslant 2\theta_L^{\min} < 2\theta_{L+1}^{\min} < 2\theta_L^{\max} < 2\theta_{L+1}^{\max} \leqslant 2\theta^{\max}$ for each L.

The function $F(2\theta)$ is easy to calculate using standard computer procedures and gives a good approximation of the experimental profile after background correction. A plot of this function against the angular variable 2θ is presented in figure 1(*a*) as an experimental curve.

5. Results

The experimental and theoretical diffraction profiles were fitted by a computer trial-and-error procedure, systematically varying the parameters $\Delta\alpha$, σ_Λ, Λ_0, η_h, σ_0^h in equation (8). The parameters b_1 and b_2 in equation (7*b*) were chosen as follows: $b_1 = \Lambda_0 - \frac{3}{2}\sigma_\Lambda$, $b_2 = \Lambda_0 + \frac{3}{2}\sigma_\Lambda$. In this way almost all modulation wavelengths which could exist in the Alnico sample are taken into account during the integration of equation (8).

In figure 1(*a*) the experimental profile in the vicinity of the (200) nodal reflection and the theoretical reflection obtained by the fitting procedure mentioned above are shown. The parameters which give the best fit are presented in table 1. The successive components of this theoretical intensity spectrum in the vicinity of the (200) nodal reflection obtained by means of equation (4) for $L = 0$ and by means of equation (5) for $|L| \leqslant 3$ are presented in figure 1(*b*). The components with $|L| > 3$ were neglected considering the small values of their amplitudes. By comparison of the experimental and theoretical diffraction profiles it is seen that a good agreement between the two was obtained, which confirms the validity of the assumed model.

In this paper two measures are introduced which characterise a scattering intensity profile: the relative half-width σ_Λ/σ_0 and the asymmetry A_L. These are defined as

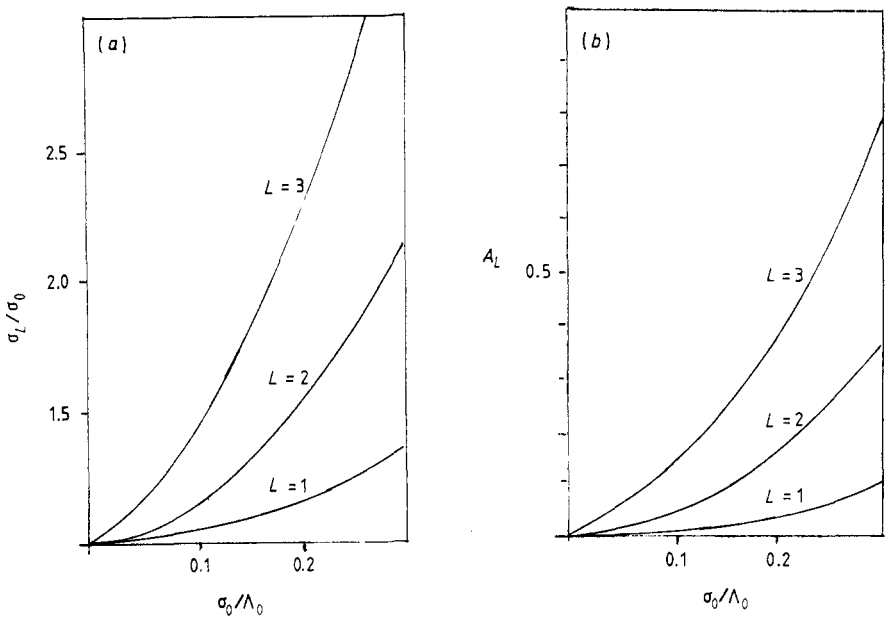

Figure 2. (*a*) The relative half-width of the first three satellite reflections plotted against the assumed modified gaussian's relative half-width in the case $\Lambda_0 = 200$ Å. (*b*) The asymmetry (defined by equation (9*b*)) of the first three satellite reflections, $L = 1, 2, 3$, plotted against the modified gaussian's relative half-width in case $\Lambda_0 = 200$ Å.

follows: let θ_1^L and θ_3^L denote the values of the angular variable θ for which the intensity of the Lth satellite reflection $I^L = 0.5I^L_{\max}$ and θ_2^L for $I^L = I^L_{\max}$ in such a way that for $L > 0$, $\theta_1 > \theta_3$ and for $L < 0$, $\theta_1 < \theta_3$:

$$\sigma_L = |\theta_1^L - \theta_3^L| \tag{9a}$$

$$A_L = (|\theta_1^L - \theta_2^L| - |\theta_2^L - \theta_3^L|)/0.5\,|\theta_1^L - \theta_3^L|. \tag{9b}$$

The values of the parameters A_L and σ_L/σ_0 were calculated as a function of σ_Λ/Λ_0 using equation (8) when the integration is taken over the interval $b_1 = \Lambda_0 - \frac{3}{2}\sigma_\Lambda$, $b_2 = \Lambda_0 + \frac{3}{2}\sigma_\Lambda$ and only Kα_1 radiation is taken into account.

Figure 2 presents the results of the calculations performed for the following values of the parameters: $L = 1, 2, 3$, $\Delta a/a = 0.014$, $\eta_h = -0.26$ and $\Lambda_0 = 200$ Å. It is seen from this figure that for every satellite reflection profile there is a monotonic increase in both the relative half-width and the asymmetry as the value of σ_Λ/Λ_0 increases. When σ_Λ/Λ_0 is held fixed, the relative half-width and the asymmetry increase with the order L of the satellite reflection. Equation 6(*b*) implies that this occurs for all values of Λ_0.

6. Conclusions

We have considered a simple model of a crystal in which coherent scattering domains exist, each of which diffracts independently the incident x-ray beam. The main properties of this model and conclusions concerning its experimental verification can be summarised as follows.

(i) The resulting diffracted intensity is a sum of partial intensities from different CSDS.

(ii) If there is a dispersion of the modulation wavelength in the sample this involves the broadening of the satellite reflections in relation to the nodal reflection. This is in agreement with remarks contained in references [2–4, 6].

(iii) The CSD model presented here enables verification of the different $N(\Lambda)$ distributions in materials and allows calculation of their parameters.

(iv) The model was verified experimentally for an Alnico sample and a modified gaussian distribution of the modulation wavelength. In this case there is a non-linear dependence between the half-widths of the satellites and their order L. The half-widths and the asymmetry of the satellites are monotonically increasing functions of the gaussian distribution $N(\Lambda)$.

(v) The considerations presented in this paper can be generalised when in each CSD the modulation wave can be described by more than one harmonic. In this case the theory for a sinusoidal modulation wave should be replaced by a general theory [4]. As a result, equation (8) will be changed appropriately, but the reasoning leading to it remains the same.

Acknowledgment

The authors are grateful to Dr T Dymkowski for supplying the samples of the Alnico alloy.

References

[1] de Fontaine D 1966 *Local Atomic Arrangements Studied by X-ray Diffraction* ed. J B Cohen and J E Hilliard (New York: Gordon & Breach)
[2] Segmuller A and Blakeslee A E 1973 *J. Appl. Crystallogr.* **6** 19–25
[3] Gaca J, Wójcik M and Sass J 1988 *Phys. Lett.* **128A** 211–6
[4] Fleming R M, McWhan D B, Gossard A G, Wiegmann W and Logan R A 1980 *J. Appl. Phys.* **51** 367–73
[5] Gyorgy E M, McWhan D B, Dillon J R Jr, Walker L R and Waszczak J V 1982 *Phys. Rev.* B **25** 6739–47
[6] McWhan D B 1985 *Structure of Chemically Modulated Films* ed. L L Chang and B C Giessen (Orlando, FL: Academic)
[7] Hillert M 1956 *DSc Thesis* Massachusetts Institute of Technology, Cambridge, MA, USA
[8] Greer A L and Spaepen F *Structure of Chemically Modulated Films* ed. L L Chang and B C Giessen (Orlando, FL: Academic)
[9] Sass J, Gaca J, Wójcik M, Dymkowski T and Kĭodaś K 1987 *14th Int. Congr. of Crystallography, Perth, Australia* Late abstr. 07 9–13
[10] Sass J, Gaca J, Wójcik M, Dymkowski T and Kĭodaś K 1988 *IEEE Trans. Magn.* **24** 1939–41
[11] Vardanyan D M, ManoukYan H M and Petrosyan H M 1985 *Acta Crystallogr.* A **41** 212–22